AAC
Journals.ASM.org

Activation of Benznidazole by Trypanosomal Type I Nitroreductases Results in Glyoxal Formation

Belinda S. Hall* and Shane R. Wilkinson

Queen Mary Pre-Clinical Drug Discovery Group, School of Biological and Chemical Sciences, Queen Mary University of London, London, United Kingdom

Benznidazole, a 2-nitroimidazole, is the front-line treatment used against American trypanosomiasis, a parasitic infection caused by *Trypanosoma cruzi*. Despite nearly 40 years of use, the trypanocidal activity of this prodrug is not fully understood. It has been proposed that benznidazole activation leads to the formation of reductive metabolites that can cause a series of deleterious effects, including DNA damage and thiol depletion. Here, we show that the key step in benznidazole activation involves an NADH-dependent trypanosomal type I nitroreductase. This catalyzes an oxygen-insensitive reaction with the interaction of enzyme, reductant, and prodrug occurring through a ping-pong mechanism. Liquid chromatography/mass spectrometry (LC/MS) analysis of the resultant metabolites identified 4,5-dihydro-4,5-dihydroxyimidazole as the major product of a reductive pathway proceeding through hydroxylamine and hydroxy intermediates. The breakdown of this product released the reactive dialdehyde glyoxal, which, in the presence of guanosine, generated guanosine-glyoxal adducts. These experiments indicate that the reduction of benznidazole by type I nitroreductase activity leads to the formation of highly reactive metabolites and that the expression of this enzyme is key to the trypanocidal properties displayed by the prodrug.

The insect-transmitted, protozoan parasites *Trypanosoma cruzi* and *Trypanosoma brucei* are the etiological agents of Chagas' disease and human African trypanosomiasis, respectively. Over 10 million people are infected by these organisms, causing around 44,000 deaths per year (40). As a result of improved surveillance, treatment, insect vector control, and housing programs, the number of new cases in areas where the diseases are endemic is on the decline, while population movement, blood transfusion, organ transplantation, and illicit drug usage have all contributed to the emergence of these infections as a problem elsewhere (3). With no immediate prospect of a vaccine, drugs are the only viable option for treatment. One therapy currently used against Chagas' disease is the nitroheterocyclic compound benznidazole. However, the use of this drug is problematic, as it can cause side effects and is potentially mutagenic, some strains are refractory to its effects, and its manufacture is currently in jeopardy (5). Additionally, benznidazole is active only against the initial acute phase of the disease, although a recent large-scale, multicenter, international trial (BENEFIT project) indicated that treatment against chronic stages is an appropriate course of action, especially for patients with cardiovascular complications (20).

Nitroheterocyclic compounds generally function as prodrugs and must undergo activation to mediate their cytotoxic effects. A key step in this process is the reduction of the nitro group, which is attached to the aromatic ring. Two classes of enzyme, the type I and type II nitroreductases, can catalyze this reaction (34). Type I nitroreductases are flavin mononucleotide (FMN) binding, NAD(P)H-dependent proteins restricted largely to prokaryotes. They mediate the transfer of 2-electrons to the target substrate, forming a nitroso intermediate, and then promote a second 2-electron reduction to generate a hydroxylamine (34, 50). This derivative can interact directly with biological macromolecules, leading to cell damage, or undergo further processing to generate cytotoxic agents (23, 36, 50). In contrast, the ubiquitous oxygen-sensitive type II nitroreductases mediate a 1-electron reduction of the nitro group, producing a nitro anion radical. In the presence of oxygen, this molecule is rapidly reoxidized back to the parent compound with the concomitant production of superoxide anions (21, 34). The resultant futile cycle can potentially cause oxidative cell damage.

Most nitroheterocyclic prodrugs can undergo both type I and type II nitroreductase activation, leading to confusion about how certain compounds mediate their cytotoxic actions. In the case of benznidazole, two mechanisms accounting for its trypanocidal activity have been proposed. The first involves a type II nitroreductase(s) generating oxidative stress in the parasite through superoxide anion formation. Indirect evidence for this pathway stems from functional studies of SODB1, a trypanosomal superoxide dismutase isoform located in the cytosol and glycosome (7, 52). *T. cruzi* and *T. brucei* parasites with genetically altered levels of SODB1 were shown previously to be more susceptible to benznidazole than controls, demonstrating that any perturbation of this enzyme leads to an imbalance of superoxide anion metabolism that is toxic to the parasite (35, 42). This peculiarity in toxicity and SODB1 levels presumably arises as cells with no or low levels of SODB1 activity are killed by superoxide anions, whereas parasites with elevated levels of the enzyme are affected by H_2O_2, the product of this dismutation reaction. Similar analyses of other trypanosomal superoxide dismutase isoforms through a loss of function or overexpression yielded recombinant cells that displayed a benznidazole sensitivity equivalent to that of controls, suggesting that superoxide production does not occur at appre-

Received 21 June 2011 Returned for modification 24 August 2011
Accepted 20 October 2011
Published ahead of print 28 October 2011

Address correspondence to Shane R. Wilkinson, s.r.wilkinson@qmul.ac.uk.
* Present address: Faculty of Health and Medical Sciences, University of Surrey, Surrey, United Kingdom.

Supplemental material for this article may be found at http://aac.asm.org/.

doi:10.1128/AAC.05135-11

ciable levels in other cellular locations (52). These findings appear to be at odds with studies that showed that *T. cruzi* parasites selected for benznidazole resistance have elevated levels of mitochondrial superoxide dismutase activity (30). However, cells selected for drug resistance also display altered expressions of several additional enzymes, including other components of the parasite's oxidative defense system, which may explain this discrepancy (28).

Intriguingly, the addition of benznidazole to *T. cruzi* extracts does not appear to trigger the production of significant levels of reactive oxygen species, suggesting that an alternative mechanism may be responsible for the trypanocidal activity of this prodrug (27). Recently, a trypanosomal nitroreductase designated NTR, with close similarity to the bacterial, oxygen-insensitive type I enzymes, was identified (53). Functional studies have clearly demonstrated that this enzyme plays a key role in nitroheterocyclic drug metabolism in both *T. cruzi* and *T. brucei*, as cells with reduced type I nitroreductase levels display resistance to various nitroheterocyclic agents, including benznidazole, while overexpression confers hypersensitivity. Consistent with this, *T. cruzi* epimastigotes selected for resistance to nitroheterocyclic drugs were found previously to have lost one copy of the chromosome carrying the *T. cruzi* NTR (*TcNTR*) gene (53). Additionally, a previously reported whole-genome "loss-of-function" screen using benznidazole against an induced *T. brucei* RNA interference (RNAi) library generated hits targeting only the *T. brucei NTR* (*TbNTR*) transcript (2). Together, these experiments implicate the trypanosomal type I nitroreductase as a key player in the activation of nitroheterocyclic agents. Here, we analyze the interaction between benznidazole and the parasite nitroreductase, showing that its major reduction product is a source of the reactive dialdehyde glyoxal.

MATERIALS AND METHODS

Parasite culturing. *T. brucei brucei* (Lister 427; clone 221a) bloodstream-form parasites were grown in modified Iscove's medium at 37°C under a 5% CO_2 atmosphere (14). A cell line (2T1) engineered to constitutively express the tetracycline repressor protein was grown in this medium, supplemented with 1 μg ml^{-1} phleomycin (1). Transformed 2T1 parasites were cultured in the presence of 2.5 μg ml^{-1} hygromycin. *T. cruzi* epimastigotes (clone MHOM/BR/78/Sylvio-X10/6) were grown in modified RPMI 1640 medium at 28°C (17).

Compounds. The compounds used in this study were obtained from the following sources: benznidazole was obtained from Simon Croft (London School of Hygiene and Tropical Medicine); pimonidazole and EF5 were obtained from Cameron J. Koch (University of Pennsylvania); metronidazole, tinidazole, secnidazole, and nimorazole were obtained from Nubia Boechat (Far Manguinhos, Rio de Janeiro, Brazil); megazol was obtained from Mike Barrett (University of Glasgow); and 6-amino PA824 was obtained from Clifton Barry III (National Institute of Allergy and Infectious Diseases) and Ujjini Manjunatha (Novartis Institute for Tropical Diseases, Singapore, Republic of Singapore). The structures are given in Fig. S1 in the supplemental material.

Antiproliferative assays. For growth inhibition assays, *T. brucei* bloodstream-form parasites (1×10^3 ml^{-1}) or *T. cruzi* epimastigotes (5×10^5 ml^{-1}) were seeded into growth medium (200 μl) containing different concentrations of the drug (53). After incubation at 37°C for 3 days (*T. brucei*) or at 27°C for 2 days (*T. cruzi*), alamarBlue (20 μl) (Invitrogen) was added to each well, and the plates were incubated for a further 8 to 16 h (*T. brucei*) or 10 days (*T. cruzi*). Cell densities were determined by monitoring the fluorescence of each culture by using a Gemini fluorescent plate reader (Molecular Devices Ltd., United Kingdom) at an excitation wavelength of 530 nm, an emission wavelength of 585 nm, and a filter cutoff at 550 nm, and the drug concentration that inhibits cell growth by 50% (IC_{50}) was established. Under these conditions, untreated controls reached a cell density of 1×10^6 to 2×10^6 *T. brucei* bloodstream-form parasites ml^{-1} or 1×10^7 to 2×10^7 *T. cruzi* epimastigotes ml^{-1}, as judged by direct counts.

Enzyme activity. Enzyme activity was measured spectrophotometrically by monitoring NADH oxidation ($\lambda = 340$ nm; $\varepsilon = 6{,}220$ M^{-1} cm^{-1}) using recombinant TcNTR and TbNTR, purified as described previously (12). A standard reaction mixture (1 ml) containing 50 mM Tris-Cl (pH 7.5), NADH (100 μM), and substrate (100 μM) was incubated at room temperature for 5 min. The background rate of NADH oxidation was determined, and the reaction was initiated by the addition of the trypanosomal enzyme (20 μg) to the mixture. Data were evaluated by nonlinear regression analysis using GraphPad Prism 5 (GraphPad Software).

Oxygen consumption assay. Oxygen consumption was monitored by using the Oxygen Biosensor system (Becton, Dickinson, and Company) (11). A standard assay mixture (200 μl) containing 50 mM Tris-Cl (pH 7.5), benznidazole (100 μM), glucose dehydrogenase (1 U ml^{-1}), and glucose (3 mM) was equilibrated at 27°C for 15 min in the presence of TcNTR (4 μg) or cytochrome P450/cytochrome P450 reductase-enriched microsomal fractions (0.1 μg) (Sigma-Aldrich). Reactions were initiated by the addition of prewarmed NAD(P)H (100 μM) to the mixture. The change in fluorescence (excitation $\lambda = 486$ nm; emission $\lambda = 620$ nm) was monitored.

Liquid chromatography (LC)/MS analysis of metabolites. The 2-nitroimidazole benznidazole (100 μM) was reduced by TcNTR (40 μg ml^{-1}) using NADH (200 μM) in 50 mM NaH_2PO_4 (pH 7.5) for 10 min at 37°C. To ensure maximal reduction, an additional aliquot of NADH (200 μM) was added to the reaction mix. After 20 min of total incubation, recombinant TbNTR was bound to Ni-nitrilotriacetic acid (NTa) (20 μl) and removed by centrifugation. Supernatants were collected and analyzed by using a series 1100 liquid chromatograph with an SL Ion Trap mass spectrometer (Agilent). Samples (20 μl) were separated on a 5-μm Hypurity Elite 15- by 2.1-mm C_{18} column (Thermo Scientific), and benznidazole-derived reduction products were eluted with a 10 to 40% acetonitrile gradient in 0.1% formic acid at a flow rate of 0.2 ml min^{-1}. Metabolites were detected by using a diode array ($\lambda = 220$, 250, 300, 340, and 450 nm), and their *m/z* values were determined by positive electrospray ionization (ESI). Positive ESI-tandem mass spectrometry (MS) was performed in automatic mode using SmartFrag for ion fragmentation. MS was carried out with a drying gas temperature of 325°C, a drying gas flow of 10 liters min^{-1}, a nebulizer gas pressure of 25 lb/in^2, and a capillary voltage of 3,500 V in full-scan mode in the *m/z* range of 50 to 400.

Glyoxal detection. Glyoxal formation by benznidazole-derived metabolites was monitored spectrophotometrically (25). A standard reaction mixture containing 50 mM NaH_2PO_4 (pH 7.5), benznidazole (200 μM), TbNTR (40 μg ml^{-1}), and NADH (0 to 800 μM) was incubated at room temperature for 24 h. Aliquots (100 μl) were then added to 25 mM Girard T reagent (900 μl) (Sigma-Aldrich) in borate buffer (pH 9.2) and incubated at room temperature for 30 min. The absorbance at 325 nm was then determined, and glyoxal levels were calculated by comparison against a standard curve.

The formation of guanosine-glyoxal adducts by benznidazole-derived metabolites was monitored by using LC/MS. A standard reaction mixture containing 50 mM NaH_2PO_4 (pH 7.5) and guanosine (100 μM) was incubated for 4 days in the presence of TbNTR (40 μg ml^{-1}), benznidazole (200 μM), and NADH (a total of 800 μM was added incrementally). Supernatants were collected and analyzed by using a series 1100 liquid chromatograph with an SL Ion Trap mass spectrometer (Agilent). Samples (20 μl) were separated on a 5-μm Hypurity Elite 15- by 2.1-mm C_{18} column (Thermo Scientific), and guanosine/guanosine-glyoxal adducts were eluted isocratically with 5% acetonitrile in 0.1% formic acid at a flow rate of 0.1 ml min^{-1}. Metabolites were detected by using

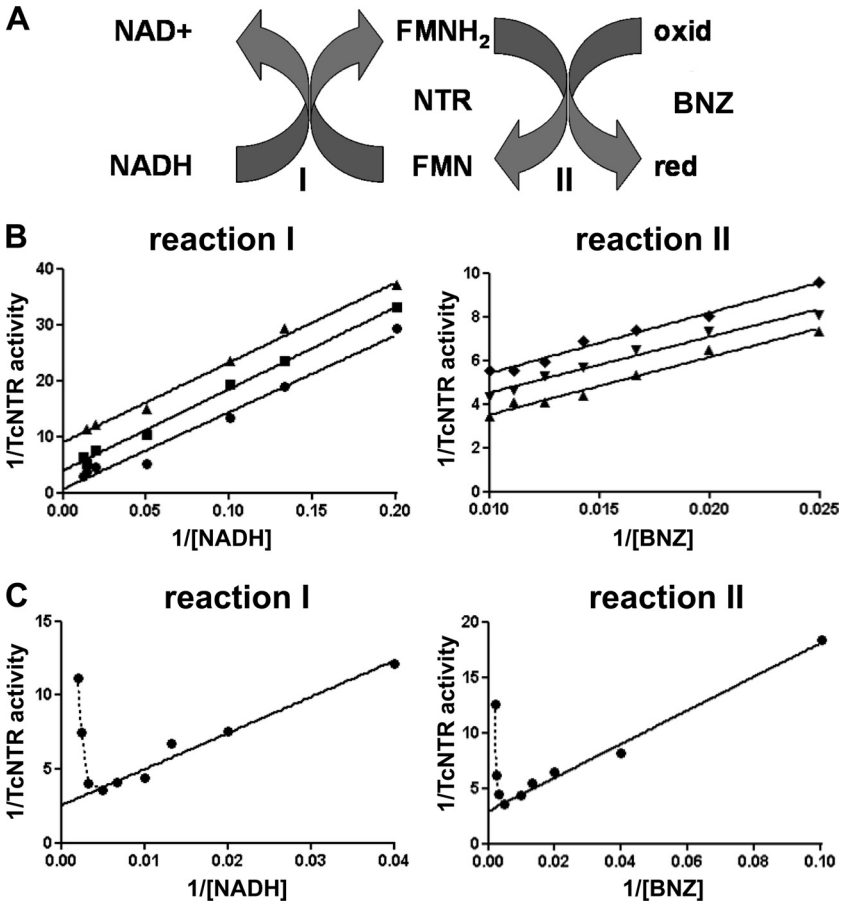

FIG 1 Investigation of the kinetic properties of trypanosomal type I nitroreductase toward benznidazole. (A) Postulated scheme for the reduction of benznidazole (BNZ) by trypanosomal type I nitroreductases (NTR) using NADH as an electron donor. "Red" represents the reduced form and "oxid" represents the oxidized form of benznidazole. The oxidized (FMN) and reduced ($FMNH_2$) forms of the flavin cofactor are indicated. (B, left) Interaction of TcNTR with NADH (reaction I). Activity was assayed by monitoring the oxidation of NADH (0 to 100 μM) in the presence of benznidazole (80 μM [▲], 90 μM [■], and 100 μM [●]) and TcNTR (20 μg). (Right) Interaction of TcNTR with benznidazole (reaction II). Activity was assayed by monitoring the oxidation of NADH (70 μM [♦], 75 μM [▼], and 80 μM [▲]) in the presence of benznidazole (0 to 100 μM) and TcNTR (20 μg). (C) Inhibition of TcNTR activity by high concentrations of NADH or benznidazole. In reaction I, a fixed concentration of benznidazole (100 μM) was reduced by TcNTR (20 μg) using various concentrations of NADH (25 to 400 μM). At high NADH levels (>200 μM), substrate inhibition was observed. In reaction II, a fixed concentration of NADH (100 μM) was oxidized by TcNTR (20 μg) using various concentrations of benznidazole (25 to 400 μM). At benznidazole concentrations above 200 μM, substrate inhibition was observed. All assays were initiated by the addition of the parasite enzyme. TcNTR activity is expressed as μmol NADH oxidized min^{-1} mg $protein^{-1}$, while [NADH] and [benznidazole] are expressed in μM. When TbNTR was used in place of TcNTR, similar enzyme kinetic profiles were observed.

a diode array ($\lambda = 260$), and *m/z* values were determined by positive ESI. Control reaction mixtures containing guanosine with and without glyoxal (200 μM) (Sigma) were carried out in parallel.

RESULTS

Metabolism of benznidazole by trypanosomal NTRs. Benznidazole toxicity depends on bioreductive activation in the target cell. Several lines of evidence have now shown that the trypanosomal type I nitroreductase plays a key role in catalyzing this reaction (see Fig. S2 in the supplemental material) (2, 53). To investigate their biochemical interaction with nitroimidazoles, recombinant versions of the TcNTR and TbNTR catalytic domains were purified following expression in *Escherichia coli* cells (12). Using NADH as an electron donor, the substrate specificity of the parasite enzymes toward various 2- and 5-nitroimidazoles was studied under aerobic conditions (Fig. 1). Only benznidazole and megazol were metabolized at an appreciable rate, with the other nitroimidazoles generating little or no activity (Table 1). To examine whether there was a correlation between enzyme activity and parasite killing, the nitroaromatic compounds were screened for trypanocidal activity against bloodstream-form *T. brucei* parasites. Out of the nine compounds analyzed, three, including benznidazole and megazol, displayed antiparasitic activity. Intriguingly, the third compound with anti-*T. brucei* properties (6-amino PA824) was not metabolized by TbNTR *in vitro*. To determine whether the parasite nitroreductase plays any role in the activation of this particular nitroimidazole in the pathogen itself, the susceptibility of bloodstream-form trypanosomes overexpressing TbNTR was investigated. Unlike benznidazole or megazol, cells with elevated TbNTR levels and controls were equally susceptible to 6-amino PA824 (see Fig. S3 in the supplemental material).

To investigate the type of kinetics that TcNTR and TbNTR display toward NADH, assays were performed in the presence of a fixed amount of parasite enzyme (20 μg) using three concentra-

TABLE 1 Reduction of nitroimidazoles by trypanosomal type I nitroreductases[a]

Compound	TbNTR			TcNTR			Trypanocidal activity (IC_{50} [μM])	
	Sp act ± SD	Apparent K_m (μM) ± SD	k_{cat}/K_m (M^{-1} s^{-1})	Sp act ± SD	Apparent K_m (μM) ± SD	k_{cat}/K_m (M^{-1} s^{-1})	*T. brucei*	*T. cruzi*
2-Nitroimidazole								
Benznidazole	419 ± 35	60 ± 13	3.0×10^3	564 ± 19	43 ± 4	6.1×10^3	22.10 ± 0.90	16.00 ± 1.00
Pimonidazole	0	—	—	—	—	—	>30	—
EF5	67 ± 8	87 ± 18	3.3×10^2	—	—	—	>30	—
5-Nitroimidazole								
Metronidazole	93 ± 9	55 ± 13	7.3×10^2	0	—	—	>40	—
Tinidazole	31 ± 3	—	—	0	—	—	>40	—
Secnidazole	26 ± 2	—	—	0	—	—	>40	—
Nimorazole	27 ± 5	—	—	0	—	—	>40	—
6-Amino PA824	0	—	—	0	—	—	3.90 ± 0.10	—
Megazol	476 ± 21	5 ± 1	4.0×10^4	1358 ± 78	22 ± 3	2.7×10^4	0.10 ± 0.01	0.46 ± 0.08

[a] The specific activities (sp act) and K_m values (± standard deviations) of TbNTR and TcNTR toward various 2- and 5-nitroimidazoles (0 to 100 μM) were determined in the presence of NADH (100 μM). Activity was followed by monitoring the rate of NADH oxidation, and the values were calculated by using an ϵ value of 6,220 M^{-1} cm^{-1}. The specific activity value is expressed as nmol NADH oxidized min^{-1} mg^{-1}, and the apparent K_m value is expressed in μM. For some compounds (benznidazole, EF5, metronidazole, and megazol), the specific activity reflects the apparent V_{max}. The catalytic efficiency (k_{cat}/K_m), expressed in M^{-1} s^{-1}, was determined, assuming one catalytic site per 30-kDa monomer. TbNTR activity toward tinadazole, secnidazole, and nimorazole was detected, but the level was too low to obtain accurate apparent K_m values, while in other cases, no activity was recorded and is expressed as 0. Dashes represent values not determined. For the trypanocidal activity, expressed as IC_{50} in μM (± standard deviation), *T. brucei* bloodstream-form and *T. cruzi* epimastigote parasites were cultured in the presence of drug (0 to 40 μM), and growth was measured by using alamarBlue (see Materials and Methods).

tions of benznidazole (80, 90, and 100 μM) against various concentrations of the reductant (0 to 100 μM). Double-reciprocal plots were linear between 10 and 200 μM NADH for all three benznidazole concentrations (reaction I) (data shown are for TcNTR, with similar results obtained for TbNTR) (Fig. 1B). The plots did not converge but yielded parallel slopes, indicative of ping-pong-type kinetics. To understand how TcNTR interacts with benznidazole, assays similar to those described above were carried out but this time using three concentrations of NADH (70, 75, and 80 μM) and varying the nitroimidazole concentration (0 to 100 μM). As with reaction I, double-reciprocal plots were linear between 10 and 100 μM benznidazole at all three NADH concentrations (reaction II) (Fig. 1B). Again, the slopes obtained for each reductant level were parallel, indicating that the interaction between the parasite enzyme and benznidazole occurs via a ping-pong mechanism. However, this type of kinetics was observed only over a limited concentration range, with substrate inhibition observed when the benznidazole or NADH level was above 200 μM (Fig. 1C).

The aerobic activation of many nitroheterocyclic compounds results in oxygen consumption and the concomitant production of reactive oxygen species. To determine whether this occurs during the TcNTR- or TbNTR-mediated reduction of benznidazole, a fluorescence-based assay using a ruthenium fluorophore was employed (11); in this system, oxygen quenches fluorescence, and an increase in the signal intensity denotes a decline in oxygen levels. In the presence of NADPH and yeast microsomes enriched for human cytochrome P450/cytochrome P450 reductase, benznidazole reduction via a type II nitroreductase activity resulted in a time-dependent increase in fluorescence, indicating that oxygen was being consumed (Fig. 2, line a). When either of the trypanosomal enzymes (TcNTR or TbNTR) was used in place of the microsomal fraction, and with NADH employed as an electron donor, no alteration in fluorescence was detected, indicating that benznidazole reduction by the parasite enzymes was not accompanied by oxygen consumption (Fig. 2, line b). This observation is consistent with the kinetic data, which gave no indication of excess NADH oxidation during the reduction of benznidazole.

Therefore, as TcNTR and TbNTR can metabolize benznida-

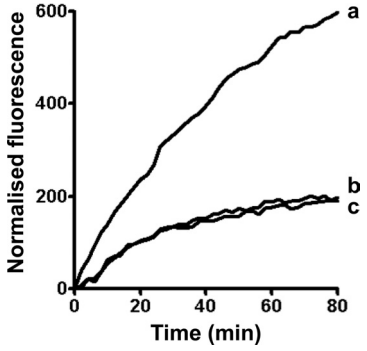

FIG 2 Oxygen consumption does not occur during benznidazole reduction by trypanosomal type I nitroreductases. Oxygen consumption was determined by using the Oxygen Biosensor system (Becton, Dickinson, and Company) (see Materials and Methods). Reaction mixtures containing benznidazole (100 μM), NAD(P)H (100 μM), and cytochrome P450 microsomes (0.1 μg) (curve a) or TcNTR (4 μg) (curve b) were incubated at 27°C for 80 min, and the change in the fluorescence of an oxygen-sensitive fluorophore was monitored. The amounts of the microsomal fraction and trypanosomal type I nitroreductase used were equivalent in their rates of NAD(P)H oxidation: the rate of NADPH oxidation by the microsomal fraction was 21 nmol NADPH oxidized min^{-1}, while the rate of NADH oxidation by TcNTR was 22 nmol NADH oxidized min^{-1}, as determined by parallel spectrophotometric assays. Control experiments lacking the enzyme or substrate were carried out in parallel (curve c shows one of several controls, all giving the same pattern). Results were normalized by the subtraction of the background signal in the absence of the enzyme and reductant. All curves are means derived from experiments performed in triplicate. When TbNTR was used in place of TcNTR, similar oxygen consumption profiles were observed.

zole under aerobic conditions via a ping-pong mechanism, without detectable oxygen consumption taking place, both trypanosomal enzymes behave as typical oxygen-insensitive, type I nitroreductases when utilizing this particular substrate.

Products arising from benznidazole reduction. The metabolism of nitroheterocyclic compounds by type I nitroreductases can lead to the formation of various end products (11, 24, 34, 50). Here, we set about to identify the nature of the benznidazole-derived metabolites following trypanosomal type I nitroreductase reduction. By using LC/MS, a series of peaks was detected (Fig. 3A). Two major products, whose mass spectra contained parent molecular ions for an $[M + H]^+$ of 265, eluted off the column as a doublet (Fig. 3B, peaks c and d). When these analytes were subject to tandem MS, they gave identical fragmentation patterns, indicating that the two starting metabolites were very similar (Fig. 3C and see Fig. S4A in the supplemental material). Fragment analysis (see Fig. S4B in the supplemental material) indicated that these two peaks corresponded to the *cis* and *trans* isomers of the 4,5-dihydro-4,5-dihydroxyimidazole derivative previously reported to be the product of the electrochemical reduction of benznidazole (Fig. 3D) (32). These isomers are formed as a result of the 4-electron reduction of benznidazole to a hydroxylamine via a nitroso intermediate that, under neutral conditions, undergoes rearrangement through a nitrenium ion to form a hydroxy derivative (Fig. 4). The hydroxy can then accept water to produce the more stable dihydro-dihyroxy end product (Fig. 3). This pathway has been shown to occur during the anaerobic reduction of 2-nitroimidazoles in mammalian systems (13).

In addition to the two isomers, four other peaks were observed. One of these peaks corresponded to unreduced benznidazole (Fig. 3A), while another, with an *m/z* of 165, corresponded to benzylamino acetamide (Fig. 3A, peak b). The two remaining peaks both had the same *m/z* value of 247 and represent the hydroxylamine and hydroxy forms (Fig. 3A, peaks a and e). Further analysis using positive and negative ESI-tandem MS failed to give a definitive identification of which peak (peak a or e) corresponded to each derivative (hydroxylamine or hydroxy). The amine derivative, a major reductive product generated by the anaerobic reductive metabolism of benznidazole in mammalian tissues (46), was not found among the NTR reductive products, although this compound was readily detectable in chemically reduced benznidazole.

Production of glyoxal and glyoxal adducts by the benznidazole reduction product. Dihydro-dihydroxyimidazoles can break down to release glyoxal (Fig. 5A), a highly reactive dialdehyde capable of forming adducts with proteins, DNA, and small molecules such as glutathione (43, 50, 51). To determine whether the TbNTR reduction of benznidazole resulted in glyoxal formation, the enzyme was incubated overnight with the drug and different concentrations of NADH. A dose-dependent production of glyoxal was detected spectrophotometrically using Girard T reagent (Fig. 5B). The release of the glyoxal moiety was time dependent and minimal when NADH or the enzyme was omitted from the reaction mixture (Fig. 5C).

Previous studies with benznidazole and other 2-nitroimidazoles have shown that the dihydro-dihydroxy reduction product can readily form adducts with guanosine, either directly or via released glyoxal (44, 47) (Fig. 6A). To determine whether the TbNTR-mediated reduction of benznidazole can lead to the formation of glyoxylated derivatives, guanosine was included in the above-described reaction mixtures. The resulting products were then analyzed by LC/MS and compared to control reaction mixtures containing untreated or glyoxal-treated purine nucleoside (Fig. 6). In reaction mixtures containing untreated guanosine, a peak eluting from the column at 3.8 min with a parent molecular ion for $[M + Na]^+$ at 306 was observed (Fig. 6B and C). When the purine nucleoside was mixed with glyoxal, two products were de-

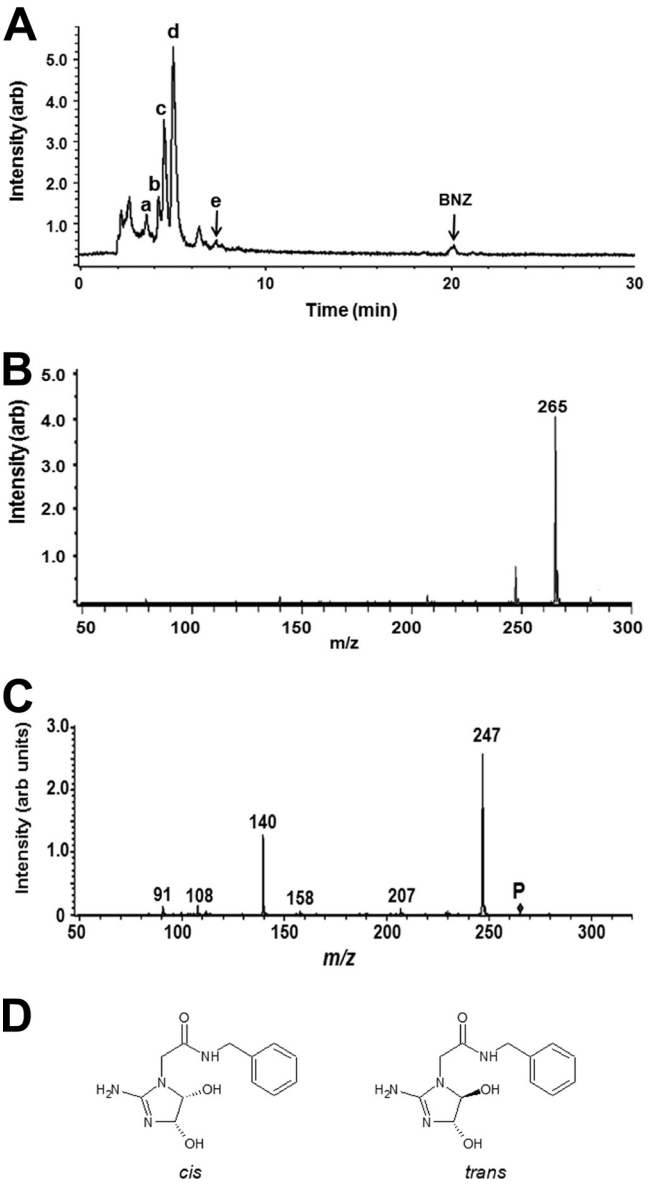

FIG 3 TcNTR reduction of benznidazole leads to formation of a dihydro-dihydroxyimidazole. (A) Representative mass spectrometry trace of the reaction products obtained after the complete reduction of benznidazole (BNZ) by TcNTR following HPLC separation. Peaks eluting at 2 to 3 min are unbound material, predominantly salts and dimethyl sulfoxide (DMSO). Peaks specifically associated with benznidazole reduction are marked (peaks a to e). (B) Positive ESI-MS for peak c from panel A. Peak d gave an identical pattern. (C) Tandem MS analysis of peak c (P) shown in panel A. An identical series of peaks was obtained when peak d was analyzed (see Fig. S3A in the supplemental material) and confirms the identity of both ions. (D) Structure of *cis* and *trans* forms of the dihydro-dihydroxy derivatives of benznidazole. When TbNTR was used in place of TcNTR, the same metabolite profile was observed. arb, arbitrary.

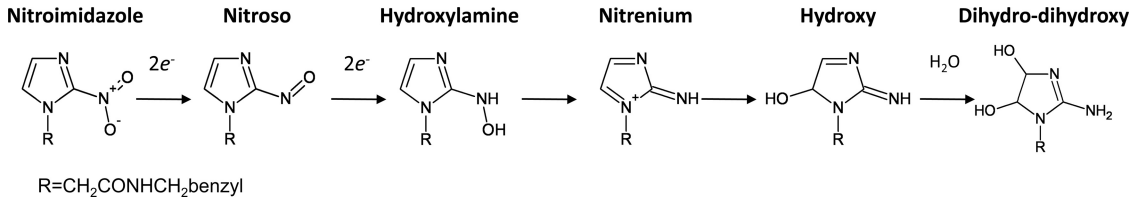

FIG 4 Outline of the reductive pathway of benznidazole. Benznidazole (nitroimidazole) is reduced to a hydroxylamine via a nitroso in a 2-step, 2-electron reaction. Under neutral conditions, the hydroxylamine rearranges to a hydroxy through a nitrenium ion intermediate. The addition of water leads to the more stable *cis* or *trans* dihydro-dihydroxy form (peaks c and d in Fig. 3). R corresponds to the benzylacetamide component of benznidazole.

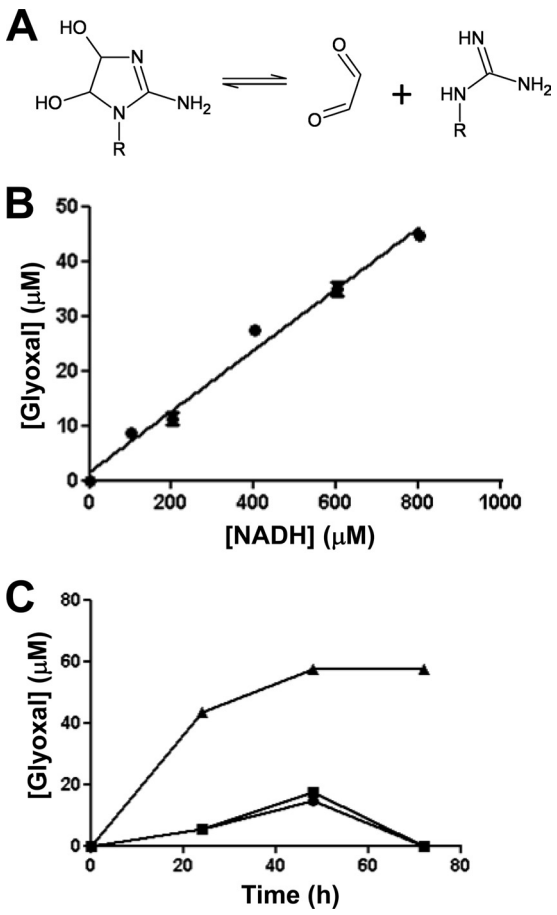

FIG 5 Release of glyoxal from the dihydro-dihydroxy form derived from benznidazole. (A) Schematic showing the release of glyoxal from dihydro-dihydroxyimidazole. (B) Spectrophotometric detection of glyoxal in reaction mixtures containing TbNTR (40 μg), benznidazole (200 μM), and various quantities of NADH (0 to 800 μM) in 1 ml 50 mM NaH_2PO_4 (pH 7.5). To detect glyoxal, an aliquot of the reaction mixture was added to a borate buffer (pH 9.2) containing Girard T reagent, and the absorbance of the mixture at 325 nm was then determined. The concentration of glyoxal in the reaction mixtures was calculated by comparison against a standard curve obtained by using pure dialdehyde, after the subtraction of blank readings from samples lacking Girard T reagent. Values are means derived from experiments performed in triplicate ± standard deviations. (C) Time-dependent production of glyoxal from benznidazole. A 1-ml reaction mixture containing benznidazole (200 μM) in 50 mM Tris-Cl (pH 7.5) was incubated at room temperature with no addition (●), NADH (total amount added, 800 μM) (■), or NADH (total amount added, 800 μM) and 4 μg TbNTR (▲). At each time point, aliquots (100 μl) were taken and assayed for the presence of glyoxal. Glyoxal concentrations were then calculated as described above.

tected as a double peak, with elution times of 3.2 and 3.3 min (Fig. 6D). These analytes both had the same *m/z* of 364 ($[M + Na]^+$) (Fig. 6E), compatible with the *cis* and *trans* forms of the guanosine-glyoxal adduct. The incubation of guanosine in the presence of TbNTR, NADH, and benznidazole resulted in several peaks (Fig. 6F). Based on elution times and MS profiles, one peak was shown to correspond to untreated nucleoside (elution time, 3.8 min), while the remaining two peaks displayed properties of the guanosine-glyoxal adducts, having elution times of 3.2 and 3.3 min and *m/z* for $[M + H]^+$ and $[M + Na]^+$ at 342 and 364, respectively (Fig. 6G). The conversion of guanosine to the guanosine-glyoxal adduct is only partial, consistent with previous reports that the process is relatively inefficient in neutral aqueous solutions (32).

The addition of the high-performance liquid chromatography (HPLC)-purified dihydro-dihydroxyimidazole did not have any significant effect on the growth of bloodstream-form *T. brucei* parasites, while exogenously added glyoxal was mildly toxic, having an IC_{50} of ~95 μM; procyclic *T. brucei* was reported previously to have an IC_{50} for methylglyoxal of ~70 μM (9). It is likely that purified dialdehyde and dialdehyde derived from dihydro-dihydroxyimidazole interact with serum proteins and thiols present in parasite growth medium as well as with parasite surface molecules. This would prevent it accessing targets that would be encountered when glyoxal is formed intracellularly and, thus, reduce toxicity. Attempts to investigate the trypanocidal activity of the other benznidazole metabolites were hampered by the instability of these compounds.

DISCUSSION

Benznidazole is a 2-nitroimidazole prodrug that has been used since the 1970s to treat patients suffering from Chagas' disease. However, its mechanism of action has remained elusive. Here, we demonstrate that benznidazole is activated by the trypanosomal type I nitroreductase, a class of enzyme present in many prokaryotes and some protozoan parasites but absent from humans. The reduction of the prodrug leads to the formation of a hydroxylamine derivative that spontaneously converts via nitrenium and hydroxy intermediates to a dihydro-dihydroxyimidazole (Fig. 3). This then dissociates to yield the cytotoxic and mutagenic agent glyoxal (Fig. 5 and 6). These findings, in conjunction with those examining the susceptibility of parasites engineered or selected to express altered levels of the type I nitroreductase (see Fig. S2 in the supplemental material) (2, 53), demonstrate that the selective toxicity of benznidazole may be attributable to the expression of this enzyme by trypanosomes and indicate that this prodrug mediates much of its antiparasitic activity through the production of cytotoxic metabolites.

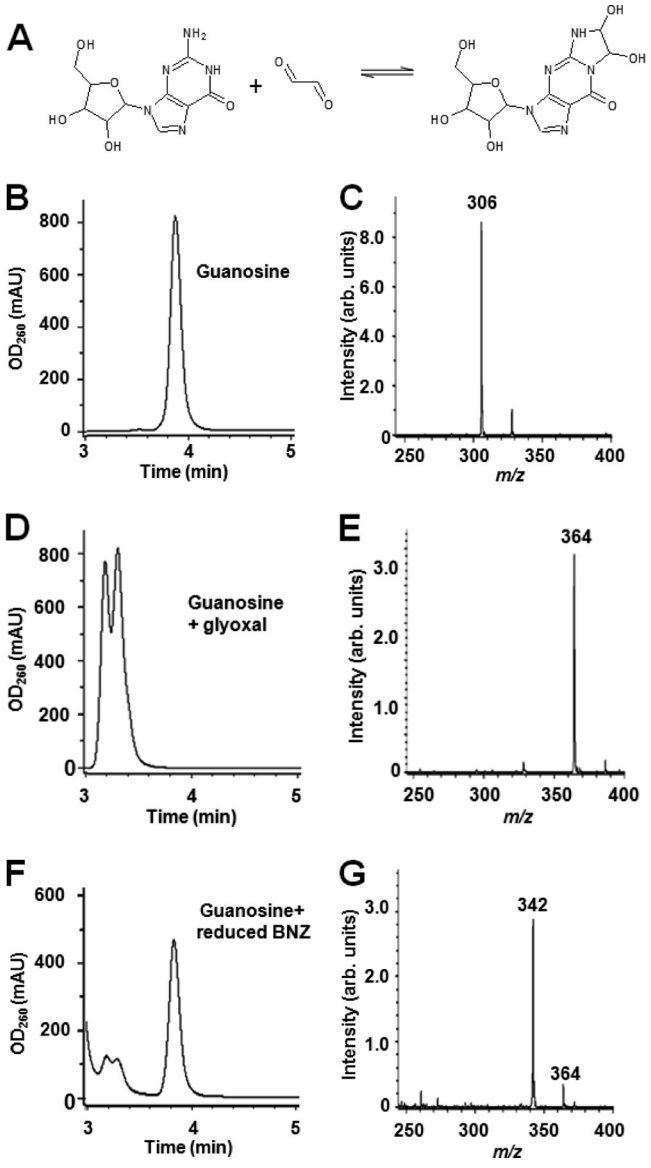

FIG 6 Formation of guanosine-glyoxal adduct by the nitroreductase-mediated reduction of benznidazole. (A) Schematic showing adduct formation from glyoxal and guanosine (32, 44). (B) HPLC trace of untreated guanosine (elution time = 3.8 min). OD_{260}, optical density at 260 nm; mAU, milliabsorbance units. (C) Positive ESI-MS profile of the peak shown in panel B. The main ion has an *m/z* value of 306 and corresponds to guanosine plus Na^+. (D) HPLC trace of guanosine-glyoxal adducts following treatment of the purine nucleobase with the purified dialdehyde. (E) Positive ESI-MS profile of the peak eluting at 3.2 min shown in panel D. The main ion associated with this peak had *m/z* values of 364, corresponding to guanosine-glyoxal plus Na^+. The second peak eluting at 3.3 min (D) had exactly the same MS profile. (F) HPLC trace of guanosine and guanosine-glyoxal adducts formed following the TbNTR-mediated reduction of benznidazole (BNZ). (G) Positive ESI-MS profile of the peak eluting at 3.2 min shown in panel F. The main ions associated with this peak had *m/z* values of 364 and 342, corresponding to guanosine-glyoxal plus Na^+ or guanosine-glyoxal plus H^+, respectively. As described above, the second peak eluting at 3.3 min in panel F had exactly the same MS profile. In panels B, D, and F, the absorbance was measured at a λ of 260 nm.

Nitroimidazoles such as the metronidazole family of antibiotics are used to treat a range of microaerophilic/anaerobic bacterial and protozoal infections. These prodrugs can be activated by two mechanisms, both involving the reduction of the conserved nitro group. In one pathway, proteins such as thioredoxin reductase, cytochrome P450 reductase, and ferredoxin promote the 1-electron reduction of the nitro substituent to yield a nitro anion radical (15, 18, 19, 49). Under normoxic conditions, the nitro anion radical can undergo futile cycling with oxygen, producing superoxide anions and regenerating the parent nitro-compound (33). This activation process is predominant in mammalian cells (27, 33). Where oxygen is limited, the nitroso form can be produced either by a further single-electron reduction step or by the interaction of two nitro anions (26). The nitroso molecule is highly reactive and can lead to cellular damage directly or indirectly through the formation a hydroxylamine derivative (16, 18). This pathway is believed to underlie the selective toxicity of nitroimidazoles against infections caused by anaerobic/microaerophilic microbes and prodrug activation in hypoxic tumors.

In contrast, nitroimidazole activation can occur via an alternative pathway, catalyzed by FMN-containing, oxygen-insensitive, type I nitroreductases (8). In this system, a series of 2-electron reductions results in the formation of the hydroxylamine derivative without the formation of the nitro anion radical. Although the aerobic reduction of nitroimidazoles by type I nitroreductases is thermodynamically unfavorable—the reduction potential (E_0) of the FMN cofactor at pH 7.0 is higher (E_0 between −90 and −290 mV) than that of many of the substrates (e.g., E_0 values for 5-nitroimidazoles range between −400 and −510 mV) (29, 47)—this system still represents a major activation mechanism of this compound class by microaerophilic microbes such as *Helicobacter* species (8).

Trypanosomes apparently lack gene homologues encoding ferredoxin and thioredoxin reductase, and while cytochrome P450 reductases are present in the parasites, their overexpression does not alter susceptibility to benznidazole (see Fig. S2 in the supplemental material). To date, the trypanosomal type I nitroreductase is the only parasite enzyme whose role in benznidazole activation has been confirmed by functional analysis (2, 53). To determine whether nitroimidazoles can act as substrates for the trypanosomal type I nitroreductases, biochemical screens were carried out (Table 1). Out of the six 5-nitroimidazoles tested, five showed little or no activity toward either of the parasite enzymes, while the sixth, megazol, generated a moderate level of activity. Similarly, of the three 2-nitroimidazoles analyzed, only benznidazole was reduced at an appreciable rate. In comparison with other nitroheterocycles, nitroimidazoles are generally poor substrates for the trypanosomal enzymes, a feature also displayed by their bacterial counterparts (12, 31). In most cases, the trypanocidal activity mirrored the biochemical screening results, with both megazol and benznidazole displaying growth-inhibitory properties (Table 1). Intriguingly, 6-amino PA824, a bicyclic 5-nitroimidazole currently under evaluation as an antitubercular therapy (39), was not metabolized by trypanosomal nitroreductases *in vitro* or *in vivo* but did have trypanocidal activity, yielding an IC_{50} against bloodstream-form *T. brucei* parasites approximately 10-fold lower than that reported previously for the lead compound PA824 (38) (Table 1 and see Fig. S3 in the supplemental material). Based on our finding and the finding that nifurtimox-resistant *T. brucei* lacks cross-resistance to PA824 (38), it is implicit that the bicyclic 5-nitroimidazole family of compounds acts by some other mechanism to mediate their antiparasitic activity.

Biochemical analyses of the interaction between TcNTR and TbNTR with NADH and benznidazole showed that both enzymes

operate through a ping-pong mechanism under aerobic conditions (Fig. 1). Unlike the other trypanocidal nitroheterocyclic drug, nifurtimox, this interaction does not result in oxygen consumption (Fig. 2) (11). The lack of a TcNTR- or TbNTR-mediated oxygen-consuming activity strongly suggests that the reduction of benznidazole does not lead to the formation of nitro and superoxide anions and is in keeping with previously reported data from work with parasite extracts (27). Instead, the metabolism of benznidazole by the trypanosomal type I nitroreductases proceeds via a series of short-lived intermediates to yield 4,5-dihydro-4,5-dihydroxyimidazole (Fig. 3). This then slowly dissociates to release glyoxal (Fig. 5). This reduction pattern is identical to that reported previously following the electrochemical reduction of benznidazole under neutral conditions and analogous to that observed during the cytochrome P450 reductase-mediated anaerobic reduction of the 2-nitroimidazole misonidazole (13, 32). Throughout this pathway, several potentially cytotoxic and mutagenic moieties are produced (Fig. 3). Because of their transient nature, we could not analyze the effect of these intermediates, but by analogy with the equivalent derivatives obtained from other nitroimidazoles, we can postulate that the hydroxylamine form of benznidazole could react with nucleic acids and proteins, while the nitrenium ion could conjugate with free thiols (16, 45). Such interactions may account for some of this prodrug's pleiotropic effects: benznidazole is mutagenic and causes a thiol depletion (4, 22). Likewise, many of these potentially trypanocidal properties could be attributed to glyoxal, the final end product of TbNTR-mediated benznidazole reduction (Fig. 5). This highly reactive dialdehyde can promote multiple deleterious effects in cells by reacting with amino acid side chains, leading to enzyme inhibition, protein cross-linking, and altered protein degradation, and can form adducts with nucleic acids, promoting DNA cross-links and mutation (43). Here, we demonstrate that glyoxal generated from benznidazole by the parasite enzyme leads to guanosine-glyoxal adducts, suggesting that part of this prodrug's trypanocidal activity may be through DNA damage via this dialdehyde (Fig. 6). However, as glyoxal release from the dihydro-dihydroxy metabolite of benznidazole is inefficient and does not account for all the DNA adducts detected by using the prodrug, the trypanocidal effects probably rely on the combined effects of several of its metabolites (32, 37, 44).

The contribution made by glyoxal to benznidazole toxicity is complicated by the presence of the glyoxalase system. This pathway functions to detoxify glyoxal, methylglyoxal, and other reactive dialdehydes before they can react with cellular targets. In mammalian cells, glutathione plays a key role in these processes, acting as a cofactor for the detoxification enzymes glyoxalases I and II (42). Both these enzymes are expressed in *T. cruzi* but depend on trypanothione rather than glutathione (9, 10). African trypanosomes lack glyoxalase I, and it is unclear whether the glyoxalase II present has any function in detoxification, but a pathway for the metabolism of dialdehydes does exist within this parasite (9, 48). The differences between kinetoplastid and mammalian glyoxalase systems have led to the suggestion that these enzymes could be viable drug targets for trypanosomal diseases (6). If glyoxal does indeed play a major role in nitroimidazole toxicity, compounds that specifically interfere with parasite detoxification pathways, in addition to any direct effect, could act synergistically with benznidazole to improve the efficacy of that drug.

We have now shown that a type I nitroreductase plays a key role in the activation of the prodrug benznidazole, resulting in the formation of several potentially cytotoxic metabolites. One of the products, glyoxal, can readily form adducts with many other biological molecules, and this may account for the pleiotropic effects observed when targeting trypanosomes using this 2-nitroimidazole.

ACKNOWLEDGMENTS

We thank John Kelly (London School of Hygiene and Tropical Medicine) for valuable discussions and for comments on the manuscript and Alan Scott and Ian Sanders (Queen Mary University of London) for their assistance with the analytical techniques.

REFERENCES

1. **Alsford S, Kawahara T, Glover L, Horn D.** 2005. Tagging a *T. brucei* rRNA locus improves stable transfection efficiency and circumvents inducible expression position effects. Mol. Biochem. Parasitol. **144**: 142–148.
2. **Baker N, Alsford S, Horn D.** 2011. Genome-wide RNAi screens in African trypanosomes identify the nifurtimox activator NTR and the eflornithine transporter AAT6. Mol. Biochem. Parasitol. **176**:55–57.
3. **Bern C, Montgomery SP.** 2009. An estimate of the burden of Chagas disease in the United States. Clin. Infect. Dis. **49**:e52–e54.
4. **Buschini A, et al.** 2009. Genotoxicity revaluation of three commercial nitroheterocyclic drugs: nifurtimox, benznidazole, and metronidazole. J. Parasitol. Res. **2009**:463575.
5. **Castro JA, de Mecca MM, Bartel LC.** 2006. Toxic side effects of drugs used to treat Chagas' disease (American trypanosomiasis). Hum. Exp. Toxicol. **25**:471–479.
6. **Chauhan SC, Padmanabhan PK, Madhubala R.** 2008. Glyoxalase pathway of trypanosomatid parasites: a promising chemotherapeutic target. Curr. Drug Targets **9**:957–965.
7. **Dufernez F, et al.** 2006. The presence of four iron-containing superoxide dismutase isozymes in trypanosomatidae: characterization, subcellular localization, and phylogenetic origin in *Trypanosoma brucei*. Free Radic. Biol. Med. **40**:210–225.
8. **Goodwin A, et al.** 1998. Metronidazole resistance in *Helicobacter pylori* is due to null mutations in a gene (*rdxA*) that encodes an oxygen-insensitive NADPH nitroreductase. Mol. Microbiol. **28**:383–393.
9. **Greig N, Wyllie S, Patterson S, Fairlamb AH.** 2009. A comparative study of methylglyoxal metabolism in trypanosomatids. FEBS J. **276**:376–386.
10. **Greig N, Wyllie S, Vickers TJ, Fairlamb AH.** 2006. Trypanothione-dependent glyoxalase I in *Trypanosoma cruzi*. Biochem. J. **400**:217–223.
11. **Hall BS, Bot C, Wilkinson SR.** 2011. Nifurtimox activation by trypanosomal type I nitroreductases generates cytotoxic nitrile metabolites. J. Biol. Chem. **286**:13088–13095.
12. **Hall BS, Wu X, Hu L, Wilkinson SR.** 2011. Exploiting the drug-activating properties of a novel trypanosomal nitroreductase. Antimicrob. Agents Chemother. **54**:1193–1199.
13. **Heimbrook DC, Sartorelli AC.** 1986. Biochemistry of misonidazole reduction by NADPH-cytochrome c (P-450) reductase. Mol. Pharmacol. **29**:168–172.
14. **Hirumi H, Hirumi K.** 1989. Continuous cultivation of *Trypanosoma brucei* blood stream forms in a medium containing a low concentration of serum protein without feeder cell layers. J. Parasitol. **75**:985–989.
15. **Hrdy I, Cammack R, Stopka P, Kulda J, Tachezy J.** 2005. Alternative pathway of metronidazole activation in *Trichomonas vaginalis* hydrogenosomes. Antimicrob. Agents Chemother. **49**:5033–5036.
16. **Kedderis GL, Argenbright LS, Miwa GT.** 1989. Covalent interaction of 5-nitroimidazoles with DNA and protein in vitro: mechanism of reductive activation. Chem. Res. Toxicol. **2**:146–149.
17. **Kendall G, Wilderspin AF, Ashall F, Miles MA, Kelly JM.** 1990. *Trypanosoma cruzi* glycosomal glyceraldehyde-3-phosphate dehydrogenase does not conform to the 'hotspot' topogenic signal model. EMBO J. **9**:2751–2758.
18. **Leitsch D, Kolarich D, Wilson IB, Altmann F, Duchene M.** 2007. Nitroimidazole action in *Entamoeba histolytica*: a central role for thioredoxin reductase. PLoS Biol. **5**:e211.
19. **Marczak R, Gorrell TE, Muller M.** 1983. Hydrogenosomal ferredoxin of

the anaerobic protozoon, *Tritrichomonas foetus.* J. Biol. Chem. **258**: 12427–12433.
20. **Marin-Neto JA, et al.** 2009. The BENEFIT trial: testing the hypothesis that trypanocidal therapy is beneficial for patients with chronic Chagas heart disease. Mem. Inst. Oswaldo Cruz **104**(Suppl. 1):319–324.
21. **Mason RP, Holtzman JL.** 1975. The mechanism of microsomal and mitochondrial nitroreductase. Electron spin resonance evidence for nitroaromatic free radical intermediates. Biochemistry **14**:1626–1632.
22. **Maya JD, et al.** 2003. *Trypanosoma cruzi*: effect and mode of action of nitroimidazole and nitrofuran derivatives. Biochem. Pharmacol. **65**: 999–1006.
23. **McCalla DR.** 1983. Mutagenicity of nitrofuran derivatives: review. Environ. Mutagen. **5**:745–765.
24. **McCalla DR, Reuvers A, Kaiser C.** 1971. Breakage of bacterial DNA by nitrofuran derivatives. Cancer Res. **31**:2184–2188.
25. **Mitchel RE, Birnboim HC.** 1977. The use of Girard-T reagent in a rapid and sensitive methods for measuring glyoxal and certain other alpha-dicarbonyl compounds. Anal. Biochem. **81**:47–56.
26. **Moreno SN, Docampo R.** 1985. Mechanism of toxicity of nitro compounds used in the chemotherapy of trichomoniasis. Environ. Health Perspect. **64**:199–208.
27. **Moreno SN, Docampo R, Mason RP, Leon W, Stoppani AO.** 1982. Different behaviors of benznidazole as free radical generator with mammalian and *Trypanosoma cruzi* microsomal preparations. Arch. Biochem. Biophys. **218**:585–591.
28. **Murta SM, et al.** 2008. Differential gene expression in *Trypanosoma cruzi* populations susceptible and resistant to benznidazole. Acta Trop. **107**: 59–65.
29. **Nivinskas H, et al.** 2001. Quantitative structure-activity relationships in two-electron reduction of nitroaromatic compounds by *Enterobacter cloacae* NAD(P)H:nitroreductase. Arch. Biochem. Biophys. **385**:170–178.
30. **Nogueira FB, et al.** 2006. Increased expression of iron-containing superoxide dismutase-A (TcFeSOD-A) enzyme in *Trypanosoma cruzi* population with *in vitro*-induced resistance to benznidazole. Acta Trop. **100**: 119–132.
31. **Olekhnovich IN, Goodwin A, Hoffman PS.** 2009. Characterization of the NAD(P)H oxidase and metronidazole reductase activities of the RdxA nitroreductase of *Helicobacter pylori.* FEBS J. **276**:3354–3364.
32. **Panicucci R, McClelland RA.** 1989. 4,5-Dihydro-4,5-dihydroxyimidazoles as products of the reduction of 2-nitroimidazoles. HPLC assay and demonstration of equilibrium transfer of glyoxal to guanine. Can. J. Chem. **67**: 2128–2135.
33. **Perez-Reyes E, Kalyanaraman B, Mason RP.** 1980. The reductive metabolism of metronidazole and ronidazole by aerobic liver microsomes. Mol. Pharmacol. **17**:239–244.
34. **Peterson FJ, Mason RP, Hovsepian J, Holtzman JL.** 1979. Oxygen-sensitive and -insensitive nitroreduction by *Escherichia coli* and rat hepatic microsomes. J. Biol. Chem. **254**:4009–4014.
35. **Prathalingham SR, Wilkinson SR, Horn D, Kelly JM.** 2007. Deletion of the *Trypanosoma brucei* superoxide dismutase gene *sodb1* increases sensitivity to nifurtimox and benznidazole. Antimicrob. Agents Chemother. **51**:755–758.
36. **Raleigh JA, Koch CJ.** 1990. Importance of thiols in the reductive binding of 2-nitroimidazoles to macromolecules. Biochem. Pharmacol. **40**: 2457–2464.
37. **Silver AR, McNeil SS, O'Neill P, Jenkins TC, Ahmed I.** 1986. Induction of DNA strand breaks by reduced nitroimidazoles. Implications for DNA base damage. Biochem. Pharmacol. **35**:3923–3928.
38. **Sokolova AY, et al.** 2010. Cross-resistance to nitro drugs and implications for treatment of human African trypanosomiasis. Antimicrob. Agents Chemother. **54**:2893–2900.
39. **Stover CK, et al.** 2000. A small-molecule nitroimidazopyran drug candidate for the treatment of tuberculosis. Nature **405**:962–966.
40. **Stuart K, et al.** 2008. Kinetoplastids: related protozoan pathogens, different diseases. J. Clin. Investig. **118**:1301–1308.
41. **Temperton NJ, Wilkinson SR, Meyer DJ, Kelly JM.** 1998. Overexpression of superoxide dismutase in *Trypanosoma cruzi* results in increased sensitivity to the trypanocidal agents gentian violet and benznidazole. Mol. Biochem. Parasitol. **96**:167–176.
42. **Thornalley PJ.** 1990. The glyoxalase system: new developments towards functional characterization of a metabolic pathway fundamental to biological life. Biochem. J. **269**:1–11.
43. **Thornalley PJ.** 2008. Protein and nucleotide damage by glyoxal and methylglyoxal in physiological systems—role in ageing and disease. Drug Metabol. Drug Interact. **23**:125–150.
44. **Varghese AJ, Whitmore GF.** 1983. Modification of guanine derivatives by reduced 2-nitroimidazoles. Cancer Res. **43**:78–82.
45. **Varghese AJ, Whitmore GF.** 1985. Properties of 2-hydroxylaminoimidazoles and their implications for the biological effects of 2-nitroimidazoles. Chem. Biol. Interact. **56**:269–287.
46. **Walton MI, Workman P.** 1987. Nitroimidazole bioreductive metabolism. Quantitation and characterisation of mouse tissue benznidazole nitroreductases *in vivo* and *in vitro.* Biochem. Pharmacol. **36**:887–896.
47. **Wardman P.** 1985. Some reactions and properties of nitro radical-anions important in biology and medicine. Environ. Health Perspect. **64**: 309–320.
48. **Wendler A, Irsch T, Rabbani N, Thornalley PJ, Krauth-Siegel RL.** 2009. Glyoxalase II does not support methylglyoxal detoxification but serves as a general trypanothione thioesterase in African trypanosomes. Mol. Biochem. Parasitol. **163**:19–27.
49. **West SB, et al.** 1982. Drug residue formation from ronidazole, a 5-nitroimidazole. I. Characterization of in vitro protein alkylation. Chem. Biol. Interact. **41**:265–279.
50. **Whitmore GF, Varghese AJ.** 1986. The biological properties of reduced nitroheterocyclics and possible underlying biochemical mechanisms. Biochem. Pharmacol. **35**:97–103.
51. **Whitmore GF, Varghese AJ, Gulyas S.** 1986. Reaction of 2-nitroimidazole metabolites with guanine and possible biological consequences. IARC Sci. Publ. **1986**:185–196.
52. **Wilkinson SR, et al.** 2006. Functional characterisation of the iron superoxide dismutase gene repertoire in *Trypanosoma brucei.* Free Radic. Biol. Med. **40**:198–209.
53. **Wilkinson SR, Taylor MC, Horn D, Kelly JM, Cheeseman I.** 2008. A mechanism for cross-resistance to nifurtimox and benznidazole in trypanosomes. Proc. Natl. Acad. Sci. U. S. A. **105**:5022–5027.